# HISTOGRAM SPECIFICATION-BASED IMAGE ENHANCEMENT FOR BACKLIT IMAGE

*Yoshiaki Ueda, Daiki Moriyama*⋆*, Takanori Koga*†*, Noriaki Suetake*‡

Fukuoka University, Izumo Murata Manufacturing Co., Ltd.⋆, Kindai University†, Yamaguchi University‡

## ABSTRACT

In this study, focusing on the fact that the intensity histogram of a backlit image shows a characteristic bimodal distribution, we propose an image enhancement method for single backlit images using histogram specification. In general, well-known histogram equalization-based techniques are powerful in image enhancement, but when simply applied to backlit images, they often change the overall appearance and also highlight unnaturalness. In the proposed method, a target shape of the intensity histogram that improves the bimodal distribution is determined, and then intensity conversion by histogram specification is conducted while preserving hue and saturation. The effectiveness of the proposed method is verified through a series of comparative experiments.

***Index Terms*—** Backlit image, image enhancement, histogram specification, bimodal distribution

## 1. INTRODUCTION

Extremely dark and bright regions are often mixed in photographs taken under backlight. As shown in Fig. 1, compared with the background overexposed (*i.e.* frontlit: F-) region, the foreground underexposed (*i.e.* backlit: B-) region becomes dark and low-contrast; it makes difficult to distinguish the details of the object. Such images frequently show an extreme bimodal histogram as shown in Fig. 1 [1].

Generally, Histogram Equalization (HE) [2] and Contrast Limited Adaptive HE (CLAHE) [3] are well-known image contrast enhancement methods. However, backlit image enhancement by these methods might be unnatural due to artifacts and over-enhancement. Multi-Scale Retinex (MSRCR) [4] can take into account the difference in intensity distribution for each local region of the image, thus it also can be applied to backlit image enhancement. However, it tends to cause halo and gray-out. Edge-preserving decomposition by Farbman *et al.* [5] tends to cause the detailed pattern to disappear due to edge-preserving smoothing. Local Laplacian Filter-based enhancement by Paris *et al*. [6] tends to enhance noise excessively in B-regions. In particular for backlit images, Kojima *et al.* proposed Stochastic Resonance-based method [7] and Wang *et al.* proposed a fusion-based one [8]. Though Li *et al.* proposed a learning-based method [9], the costs of learning data collection and calculation are high.

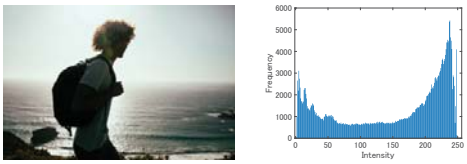


**Fig. 1**. Backlit image and its bimodal histogram.

In this study, we propose a straightforward image enhancement method for single backlit images based on intensity conversion with hue and saturation preservation. In the intensity conversion, the proposed method performs histogram specification using a triangular-shaped unimodal target histogram. This aims at improving the bimodal distribution of the intensity histogram of a backlit image. Furthermore, the improved intensity channel is blended with the input image's one to correct the contrast of the intermediate region. Finally, the overall RGB channels' conversion results are calculated while preserving the original hue and saturation in constant-hue planes. Through these processes, a high-quality backlit image enhancement is realized. The effectiveness of the proposed method is verified through a comparative experiment.

## 2. PROPOSED METHOD

First, the histogram of an input backlit image is divided into F- and B-regions using a threshold given by linear discriminant analysis (LDA) [10]. Then a triangular target histogram is obtained using the threshold as shown in Fig. 2(a). Basically, the proposed method improves the intensity of a backlit image by histogram specification using this target. In this regard, such simple triangular target shape may cause unbalanced conversion between F- and B-regions. To cope with this problem, two modified targets shown in Fig. 2(b) (Target 1) and Fig. 2(c) (Target 2) are used. Target 1 is obtained by adjusting the ratio of the B- and F-regions to be the same as the area ratio of the input image. The F-region of Target 2 is the same as the shape of the input image's one.

To conduct intensity conversion based on histogram specification, an intensity image $I_{ij}$ of an input color image $\boldsymbol{x}_{ij} = (x_{ij}^R, x_{ij}^G, x_{ij}^B)$ is calculated as follows:

$$I_{ij} = (x_{ij}^R + x_{ij}^G + x_{ij}^B)/3, \tag{1}$$

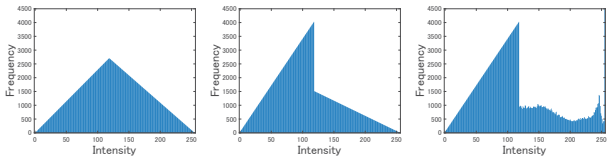


**Fig. 2**. Three types of target histograms. (a) Basic shape, (b) Target 1, (c) Target 2.

where $i$ and $j$ are coordinates in the image. Letting $h^{\mathrm{tar}}$ be a target histogram, a result of histogram specification is calculated as follows:

$$I_{ij}^{HS} = \inf\{z | H(I_{ij}) \leq H^{\mathrm{tar}}(z)\}, \tag{2}$$

where $H$ and $H^{\mathrm{tar}}$ are the normalized cumulative histogram of an input image and that of a target histogram, respectively. Then, to compensate the low contrast intermediate values caused by histogram specification, the following alpha blending is calculated:

$$I'_{ij} = \alpha I_{ij}^{HS} + (1-\alpha) I_{ij}, \tag{3}$$

$$\alpha = \min\left\{1, \left|\frac{M_{ij} - \bar{I}}{\bar{I}}\right|\right\}, \tag{4}$$

where $M_{ij}$ is a Gaussian-filtered version of $I_{ij}$ with radius of $r$, and $\bar{I}$ is a mean of $I_{ij}$. Now, using a desirable conversion coefficient obtained by dividing $I'_{ij}$ by $I_{ij}$, an intensity conversion result $\boldsymbol{x}'_{ij}$ of an input image $\boldsymbol{x}_{ij}$ is calculated as follows:

$$\boldsymbol{x}'_{ij} = \frac{I'_{ij}}{I_{ij}} \boldsymbol{x}_{ij}. \tag{5}$$

Since this conversion simply multiplies the input image by a constant, it satisfies the hue preservation conditions propounded by Naik *et al.* [11].

Figure 3 shows an example of saturation preservation to prevent changes in vividness. A constant-hue plane in an RGB color space contains three points, $K = (0,0,0)$, $W = (255,255,255)$, and $\boldsymbol{x}_{ij}$. In Fig. 3(a), $d_{ij}$ and $d'_{ij}$ are the saturations of $\boldsymbol{x}_{ij}$ and $\boldsymbol{x}'_{ij}$, respectively. A saturation $d_{ij}$ is given as follows:

$$d_{ij} = \sqrt{\frac{(x_{ij}^R - x_{ij}^G)^2 + (x_{ij}^G - x_{ij}^B)^2 + (x_{ij}^B - x_{ij}^R)^2}{3}}. \tag{6}$$

Finally, a hue-and-saturation-preserving enhancement result $\boldsymbol{x}''_{ij}$ is obtained by finding out a point with an intensity $I'_{ij}$ and a saturation $\boldsymbol{x}''_{ij}$ in the plane as shown in Fig. 3(b).

## 3. EXPERIMENTS

To verify the effectiveness of the proposed method, a comparative experiment was conducted for the test images shown in

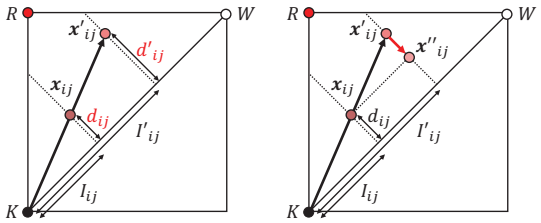


**Fig. 3**. Saturation preservation in an constant-hue plane. (a) Saturations of $\boldsymbol{x}_{ij}$ and $\boldsymbol{x}'_{ij}$, (b) Saturation preservation.

Fig. 4. CLAHE, MSRCR, HE, Farbman, Paris, and Wang are used as comparative methods. In the proposed method, the parameter $r$ was set to be 10% of the image's short side. For the parameters of the comparative method, the values shown in each paper were used. The quantitative evaluation was conducted with Lightness Order Error (LOE) [12–14], histogram entropy, and Natural Image Quality Evaluator (NIQE) [15]. The LOE is calculated as follows:

$$LOE = \frac{1}{m}\sum_{p=1}^{m}\sum_{q=1}^{m} U(\boldsymbol{L}(p), \boldsymbol{L}(q)) \oplus U(\boldsymbol{L}'(p), \boldsymbol{L}'(q)), \tag{7}$$

where $m$ is the number of pixels, $p$ and $q$ are the pixel indices, $\boldsymbol{L}(p)$ and $\boldsymbol{L}'(p)$ are the maximum RGB values in the input and output image, respectively. The function $U(s,t)$ is 1 if $s \geq t$, and 0 otherwise. The LOE indicates the difference between the order of the pixel values of an original image and that of a processing result; the smaller the value, the better the result. Histogram entropy is an index of the contrast of an image, and the larger the value, the higher the contrast and the better the result. Each region's histogram entropy is calculated using the threshold obtained by LDA. The NIQE is blind image quality assessment algorithm, and the smaller the value, the better the result.

Figures 5 and 6 are examples of processing results. Though the results of CLAHE show the improved visibility in both B- and F-regions, the unnaturalness due to overemphasis is noticeable. The significantly reduced saturation is conspicuous in the result of MSRCR shown in Fig. 5(c). In Fig. 6(c), the visibility in the B-region is improved, while it in the F-region is reduced. The results of HE show the increased intensity in the B-region; the entire image is highly visible. However, in Fig. 6(d), the visibility is not significantly improved. In the results of Farbman's method, not much improved visibility is shown, and fine patterns are lost due to edge preserving smoothing. The results of Paris's method show the improved visibility in the B-region; the vividness and details are emphasized. However, the slight intensity change in the flat part is overemphasized. In the results of Wang's method, the entire image is highly visible. However, in Fig. 5(g), the vividness of the clothes increased. In the processing results of the proposed method (Target 1),

**Fig. 4**. Test images. Image 1 to 7 are shown from left to right.

**Table 1**. Lightness order error (LOE) for the test images.

| | CLAHE | Farbman | HE | MSRCR | Paris | Wang | Prop. (Target 1) | Prop. (Target 2) |
|---|---|---|---|---|---|---|---|---|
| Average | 40187 | 20008 | 9243 | 58352 | 21995 | 21550 | 9980 | **5144** |

**Table 2**. Histogram entropy (B-region) for the test images.

| | Original | CLAHE | Farbman | HE | MSRCR | Paris | Wang | Prop. (Target 1) | Prop. (Target 2) |
|---|---|---|---|---|---|---|---|---|---|
| Image 1 | 6.11 | **7.00** | 6.09 | 5.86 | 6.40 | 6.30 | 6.47 | 6.35 | 6.35 |
| Image 2 | 6.39 | **7.22** | 6.54 | 6.35 | 6.90 | 6.49 | 6.80 | 6.54 | 6.54 |
| Image 3 | 6.38 | **7.18** | 6.19 | 6.27 | 5.96 | 6.49 | 6.57 | 6.63 | 6.63 |
| Image 4 | 6.29 | **7.34** | 6.22 | 6.16 | 6.38 | 6.70 | 6.76 | 6.62 | 6.62 |
| Image 5 | 6.85 | **7.74** | 6.69 | 6.71 | 7.19 | 6.98 | 7.17 | 6.84 | 6.84 |
| Image 6 | 6.86 | **7.36** | 7.01 | 6.37 | 6.85 | 7.24 | 7.08 | 6.79 | 6.79 |
| Image 7 | 4.83 | 6.03 | 4.66 | 4.64 | **6.68** | 5.70 | 5.98 | 5.86 | 5.86 |
| Average | 6.24 | **7.12** | 6.20 | 6.05 | 6.62 | 6.56 | 6.69 | 6.52 | 6.52 |

**Table 3**. Histogram entropy (F-region) for the test images.

| | Original | CLAHE | Farbman | HE | MSRCR | Paris | Wang | Prop. (Target 1) | Prop. (Target 2) |
|---|---|---|---|---|---|---|---|---|---|
| Image 1 | 6.77 | 6.96 | 6.67 | 6.63 | 5.02 | **7.12** | 6.72 | 6.73 | 6.77 |
| Image 2 | 6.98 | **7.38** | 7.15 | 6.20 | 6.51 | 7.06 | 7.11 | 6.84 | 6.98 |
| Image 3 | 6.41 | 6.55 | 6.44 | 6.09 | 4.69 | **6.91** | 6.49 | 6.22 | 6.41 |
| Image 4 | 6.20 | 6.42 | 6.15 | 5.73 | 5.19 | **6.77** | 6.26 | 6.03 | 6.20 |
| Image 5 | 6.13 | **6.40** | 5.92 | 5.88 | 4.61 | 6.19 | 6.38 | 6.33 | 6.13 |
| Image 6 | 6.60 | **7.02** | 6.43 | 6.44 | 5.41 | 6.48 | 6.86 | 6.61 | 6.60 |
| Image 7 | 6.98 | **7.18** | 6.73 | 6.90 | 5.50 | 7.04 | 6.88 | 6.60 | 6.98 |
| Average | 6.58 | **6.85** | 6.50 | 6.27 | 5.28 | 6.80 | 6.67 | 6.48 | 6.58 |

**Table 4**. Natural image quality evaluator (NIQE) for the test images.

| | Original | CLAHE | Farbman | HE | MSRCR | Paris | Wang | Prop. (Target 1) | Prop. (Target 2) |
|---|---|---|---|---|---|---|---|---|---|
| Image 1 | 3.93 | 3.99 | 6.02 | 3.52 | **3.44** | 5.21 | 4.36 | 3.75 | 3.79 |
| Image 2 | 2.74 | 2.87 | 2.84 | 2.42 | **2.30** | 3.15 | 2.79 | 2.33 | 2.35 |
| Image 3 | 4.13 | 4.19 | 4.97 | 3.98 | 3.85 | 3.59 | **3.34** | 3.73 | 3.88 |
| Image 4 | 2.07 | 2.09 | 3.35 | 1.96 | 2.04 | 2.67 | 2.13 | 2.02 | **1.92** |
| Image 5 | 3.46 | 3.60 | 3.30 | **3.12** | 3.63 | 3.60 | 3.39 | 3.20 | 3.37 |
| Image 6 | 2.65 | 2.78 | 3.59 | 2.62 | 2.82 | 2.98 | 2.92 | 2.51 | **2.47** |
| Image 7 | 2.67 | 2.66 | 4.89 | 2.45 | 2.51 | 2.93 | 2.47 | 2.44 | **2.35** |
| Average | 3.09 | 3.17 | 4.14 | 2.87 | 2.94 | 3.45 | 3.06 | **2.85** | 2.88 |

the visibility of the B-region is improved. However, since the intensity of the B-region is slightly reduced; the contrast is reduced. Even in the processing results of the proposed method (Target 2), the visibility of the B-region is improved. Further-


**Fig. 5**. Resulting images. (a) Original, (b) CLAHE, (c) MSRCR, (d) HE, (e) Farbman, (f) Paris, (g) Wang, (h) Proposed (Target 1), (i) Proposed (Target 2).


**Fig. 6**. Resulting images. (a) Original, (b) CLAHE, (c) MSRCR, (d) HE, (e) Farbman, (f) Paris, (g) Wang, (h) Proposed (Target 1), (i) Proposed (Target 2).

more, since the intensity of the B-region is not changed; the contrast of the entire image is high.

Tables 1–4 show the results of the quantitative evaluation. The best and the second-best scores are shown in bold and are underlined, respectively.

Table 1 shows the average LOE scores for test images. Here, each LOE score for test image is omitted to save the space. The comparative methods show the large LOE scores overall. In contrast, HE and the proposed method show the small LOE scores.

Tables 2 and 3 show the histogram entropies for each B- and F-region. The results of CLAHE, MSRCR, Paris, Wang, and Prop. tend to show the higher histogram entropies in B-region. CLAHE, Paris, and Wang show higher histogram entropy than original image in F-region. The histogram entropies tend to decrease in the results of F-region processing by the proposed method (Target 1). Therefore, for the F-region, it is better to preserve the intensity completely by using a histogram with the same shape as the original image (*i.e.* Target 2).

Table 4 shows the NIQE for each image. The results of HE and proposed methods are tend to show the lower scores and it indicates that the naturalness of the resulting images are higher than other comparative methods.

The above results show that the proposed method is suitable for natural enhancement of single backlight images.

## 4. CONCLUSIONS

In this study, we proposed a straightforward backlit image enhancement method realized by intensity conversion with hue-and-saturation-preservation. The key idea is to convert the intensity to improve the bimodal histogram as much as possible using histogram specification based on a unimodal triangular-shaped target histogram. In the experiment, we conducted comparative evaluation with multiple methods, and showed the effectiveness of the proposed method.

A future task is to suppress noise enhancement to improve the image enhancement quality.

## 5. REFERENCES


[1] J. Shin, H. Oh, K. Kim, and K. Kang, "Automatic image enhancement for under-exposed, over-exposed, or backlit images," *Electronic Imaging*, vol. 2019, no. 14, pp. 088–1–088–5, 2019.

[2] T. Acharya and A. K. Ray, *Image Processing - Principles and Applications*, Wiley-Interscience, USA, 2005.

[3] K. Zuiderveld, *Contrast Limited Adaptive Histogram Equalization*, pp. 474–485, Academic Press Professional, Inc., USA, 1994.

[4] D. J. Jobson, Z. Rahman, and G. A. Woodell, "A multiscale retinex for bridging the gap between color images and the human observation of scenes," *IEEE Transactions on Image Processing*, vol. 6, no. 7, pp. 965–976, 1997.

[5] Z. Farbman, R. Fattal, D. Lischinski, and R. Szeliski, "Edge-preserving decompositions for multi-scale tone and detail manipulation," *ACM Trans. Graph.*, vol. 27, Aug. 2008.

[6] S. Paris, S. W. Hasinoff, and J. Kautz, "Local laplacian filters: edge-aware image processing with a laplacian pyramid.," *ACM Trans. Graph.*, vol. 30, no. 4, pp. 68, 2011.

[7] N. Kojima, B. Lamsal, N. Matsumoto, and M. Yamashiro, "Proposing autotuning image enhancement method using stochastic resonance," *Electronics and Communications in Japan*, vol. 102, no. 4, pp. 35–46, 2019.

[8] Q. Wang, X. Fu, X. Zhang, and X. Ding, "A fusion-based method for single backlit image enhancement," in *2016 IEEE International Conference on Image Processing (ICIP)*, Sep. 2016, pp. 4077–4081.

[9] Z. Li and X. Wu, "Learning-Based Restoration of Backlit Images," *IEEE Transactions on Image Processing*, vol. 27, no. 2, pp. 976–986, Feb. 2018.

[10] N. Otsu, "A threshold selection method from gray-level histograms," *IEEE transactions on systems, man, and cybernetics*, vol. 9, no. 1, pp. 62–66, 1979.

[11] S. K. Naik and C. A. Murthy, "Hue-preserving color image enhancement without gamut problem," *IEEE Transactions on Image Processing*, vol. 12, no. 12, pp. 1591–1598, Dec. 2003.

[12] Z. Ying, G. Li, Y. Ren, R. Wang, and W. Wang, "A new low-light image enhancement algorithm using camera response model," in *2017 IEEE International Conference on Computer Vision Workshops (ICCVW)*, Oct. 2017, pp. 3015–3022.

[13] S. Wang, J. Zheng, H. Hu, and B. Li, "Naturalness preserved enhancement algorithm for non-uniform illumination images," *IEEE Transactions on Image Processing*, vol. 22, no. 9, pp. 3538–3548, Sep. 2013.

[14] X. Guo, Y. Li, and H. Ling, "Lime: Low-light image enhancement via illumination map estimation," *IEEE Transactions on Image Processing*, vol. 26, no. 2, pp. 982–993, Feb. 2017.

[15] A. Mittal, R. Soundararajan, and A. C. Bovik, "Making a 'completely blind' image quality analyzer," *IEEE Signal Processing Letters*, vol. 20, no. 3, pp. 209–212, March 2013.